Available online at www.sciencedirect.com

SciVerse ScienceDirect

Procedia Engineering 36 (2012) 355 – 359

Procedia Engineering

www.elsevier.com/locate/procedia

IUMRS-ICA 2011

Study of the Ti-20 wt. % Mo Composite Coating Prepared by Laser Cladding

Rongjuan Yang[a], Zongde Liu[a,b,]*, Guang Yang[a], Weiyu Ren[a]

[a]*Key Laboratory of Condition Monitoring and Control for Power Plant Equipment of Ministry of Education, North China Electric Power University, Beijing 102206, China*

[b] *Suzhou Institute of Research, North China Electric Power University, NO.188, Renai Road, Xietang area, Suzhou 215123, China*

Abstract

Laser surface cladding was applied on low carbon steel to improve its surface properties. Mixed Mo and Ti powders with a Ti-to-Mo mass ratio of 4:1 were put onto the low carbon steel and subsequently treated by laser beam. The microstructure and composition modifications in the surface layer were carefully investigated by using SEM, EDX and XRD, respectively. A Ti-Mo intermetallic compound layer with thickness of similar to 300 μm was formed on low carbon steel. The bonding between the coating layer and substrate is good and the diffusion occurs in the interface between them. From the results it is very clear that the phases in the composites coatings are composed of β-Ti phase and Fe_2Ti phases. The micro hardness of the coating reaches to above $HV_{0.5}$ 900. The improvement of the hardness of the coating on low carbon steel has been realized. Preliminary electrochemical studies have indicated Ti-Mo exhibits excellent corrosion resistance in 0.5M NaCl solution.

Keywords: Ti-Mo; compsite coating; laser cladding; eletrochemical; micro-hardness

1. Introduction

As is well known, titanium and its alloys have received much attention in various machinery, energy and transportation systems because they have good corrosion resistance, a light density, and excellent balance of mechanical properties [1-3]. In accordance with the background on titanium, most research on titanium alloys (α alloys, α+β alloys, and β alloys) is done by focusing on α+β titanium alloys such as TC4 [4], but β titanium alloys (composed of alloying stabilizers such as Nb, Ta, Zr, Mo, and Sn) are more

* Corresponding author. Tel.: +86-10-6177-2291; fax: +86-10-6177-2812.
E-mail address: lzd@ncepu.edu.cn.

1877-7058 © 2012 Published by Elsevier Ltd. Open access under CC BY-NC-ND license.
doi:10.1016/j.proeng.2012.03.052

generally developed because it possesses pronounced enhanced properties such as lower elasticity modulus, greater strength and better corrosion resistance when compared with α + β type alloys [5][6].

In recent years, Ti-Mo alloys employed as biomaterials have been studied with emphasis on their microstructure and mechanical properties [7-12]. However, so far, there are few studies on dealing with Ti–Mo alloys and their potential use as the coating. Considering that the fact that when the Mo content increased to 10 wt.% or higher, only the β phase was formed [8], So in the present study, we applied laser cladding methods to prepare the binary Ti–Mo alloys with 20 wt.% Mo contents composite coating on the plain steel substrate. The microstructure and the chemical composition of the phases obtained at the surface were investigated and electrochemical characterizations were determined.

2. Experimental details

2.1 Sample preparation and laser clad treatment

A 20mm_20mm_10mm plate of commercial low carbon steel (composition C 0.17 wt.%, Si 0.27 wt. %, Mn 0.505 wt.%, Fe balance) was used as substrate for laser cladding. Prior to the laser treatment, mixed 99.9% pure titanium and 99.9% pure molybdenum powders with a Ti-to-Mo mass ratio of 4:1 which were mixed in a ball mill and dried in a drying oven for 24h. The total depth of the powder layer is around 500 μm. In the scanning treatment, a YAG pulse laser was adopted coaxially blown pure argon (99.99%) used as shielding gas to protect the molten pool from oxidation by atmospheric air. For the present study, the optimal processing parameters are: laser output power 600-700 W, diameter of the laser spot 3 mm, traverse speed 3.5 mm/s, gas flow rate 15 L/s, and overlapped rate 30%, respectively.

2.2 Coating analysis

The microstructures and the phases of the prepared coatings were characterized by using a scanning electron microscope (SEM) with an electron dispersion X-ray spectroscopy (EDX) and X-ray diffraction (XRD) facility with CuKα radiation. The Vickers microhardness measurements were performed at 500g loads for 15s on the cross-section of coatings. The treated samples were polished before the indentations.

2.3 Electrochemical polarization experiments

The electrochemical polarization test was carried out using an electrochemical workstation at 20℃ by a standard three electrode configuration. The laser treated specimens are completely immersed into a beaker containing 200 ml of 0.5 M NaCl under open air environment. For comparison, an untreated low carbon steel sample was also prepared. The tested parameters are: the exposure area of the test surface of the specimen 1.5 cm^2, the scan rate 0.3 mV/s.

3. Results and Discussion

3.1 Microstructure of laser clad coatings

Fig. 1(a) is SEM morphology of cross-section of the Ti-Mo laser cladding coating. An even intermetallic compounds layer about 300 μm thick is free from pores and cracks through the whole section of the Ti-Mo coating and no interval can be observed at the interface between the coating and the substrate, which indicates that there is a highly dense coating and good interface bonding. For better visualization, the SEM micro-graphs and the depth profiles of Ti, Mo, Fe were overlapped and are

presented in Fig. 1(b). The line scanning position is indicated by the yellow straight line. From the scanning profile, it can be clearly seen that the Fe (green line) content gradually increases from the coating side through the interface to the substrate side, while Ti (blue line) content gradually increases from the substrate side through the interface to the coating side, The same trends can be seen in the Mo (red line) content, showing that an inter-diffusion layer was formed at the interface between the coating and the substrate. Moreover, Ti can produce intermetallic compounds with steel substrate, to cause substrate and interlayer good combination.

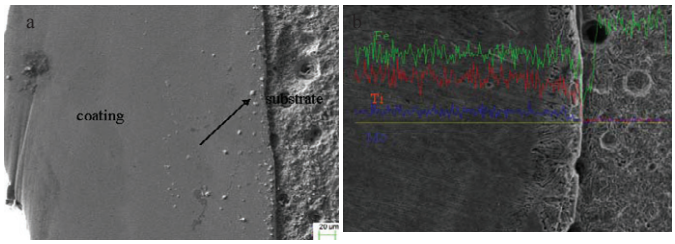

Fig.1. (a) The SEM image of the coating/substrate interface, (b) The elemental distribution pattern of the coating/substrate interface.

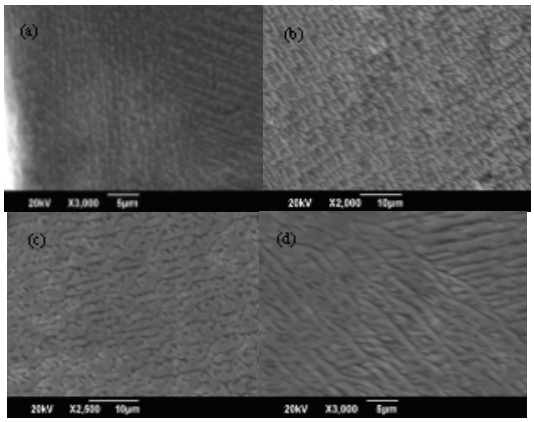

Fig.2. SEM images of laser clad layer at different zones (a, b, c, d) (a) Top surface; (b) Subsurface at about 200μm; (b) Subsurface at about 300μm ;(d) Subsurface at melt/substrate interface.

As a result of the temperature gradient and cooling rate is different in the different depth, it is seen from the picture that crystal grain size and shape varies with the depth changing. Fig.2 shows the bright gray eutectic phase very similar in morphology and distribution in the 4 zones. The compositions of the gray phase in the 4 zones are no differences in chemical composition as determined by SEM EDS analysis is (wt.%): 69.43 Fe, 22.59 Ti, 7.82 Mo, 0.16 C, which indicates that they are mainly composed of Fe_2Ti and β-Ti. This is in accordance with XRD result, the coating is diluted obviously by the substrate. As shown in Fig. 2(a) and (b), the regions with the gray appearance in the matrix was solidified first, while the darker inter-grain regions solidified later which made up primarily of β-Ti. The top surface and subsurface at about 200μm of the coating have a similar matrix structure, compared with the crystal grain in the surface, the crystal grain in the middle of the coating is obvious fine. For the subsurface at about 300μm of the coating exhibits a composite microstructure with a micrometer-sized dendrite solid solution phase dispersed in a Ti matrix. As shown in Fig.2(c). Fig. 2(d) shows SEM morphology of the bonding region between the coating and the substrate. In this area, the phases are coarsening dendrites. This shows

that the cooling rate, which is much lower for the bonding region between the coating and the substrate than for the subsurface at about 300 μm of the coating, has a significant effect on the solidified microstructure. To sum up, it is concluded that the Ti-Mo coating was formed as small particles on the top of the substrate and it then grew, covering the substrate surface during the following deposition process.

3.2 X-ray diffraction phase analysis

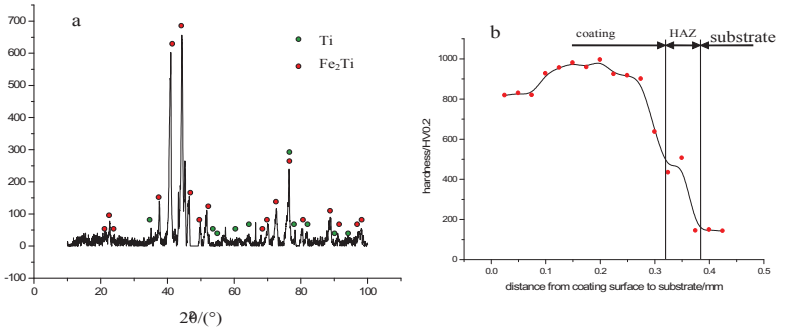

Fig. 3(a), X-ray diffraction pattern of Ti-Mo composites; (b), Microhardness profile on cross-section of Ti-Mo composites.

The X-ray analysis shown in Fig. 3(a) indicates the presence of λ (Fe_2Ti) phases in the Ti-Mo laser cladding coating on the low carbon steel. That is mostly because Ti in the original powder material can easily produce intermetallic compounds (Fe_2Ti) with steel substrate. In addition, diffraction peaks of pure Ti phase are also found, indicating that a Ti layer has been deposited on low carbon steel by laser cladding. It is obvious that diffraction peaks are broadened due to the fine grain size of Ti-Mo laser cladding coating. However, XRD analysis does not show the occurrence of Mo. This is mainly due to the fact that when the Mo content increased to 10 wt.% or higher, only the retained β phase was observed in the XRD patterns [8]. In other words, Mo stays mainly in the β-Ti so that the Mo was no detected by XRD.

3.3 Cross section microhardness of laser clad layer

As shown in Fig. 3(b), the Ti-Mo alloys (containing 20 wt.% Mo) had much higher microhardness values (about 950 $HV_{0.5}$) than that of the low carbon steel about (180 $HV_{0.5}$). That means the microhardness is enhanced about 4.5 times. It is also seen from Fig.4 that the hardest area is in the midst of the coating. The value of microhardness in the coating increases from 800 $HV_{0.5}$ to 1000 $HV_{0.5}$, then decreases gradually when approaching the substrate. As the documents [13] mentioned, the reason is that grain size and crystal structure/phase can affect the Vickers hardness of the alloy.

3.4 Corrosion property

The corrosion current density and the corrosion potential of the Ti-Mo coated sample and uncoated low carbon steel are shown in Table 1. It can be seen from Table 1 that the Ti-Mo coated sample has much lower corrosion current density (1.95×10^{-5}) than that of uncoated low carbon steel (1.16×10^{-4}). Namely, after laser cladding, the corrosion current density increases by an orders of magnitude. Similarly,

the corrosion potential of the Ti-Mo coated sample (−0.351 V) is on the top of uncoated low carbon steel (−0.66 V). As suggested above the corrosion resistance of low carbon steel has been improved by the Ti-Mo laser cladding.

Table1. The corrosion current density and the corrosion potential for low carbon steel and Ti-Mo coated sample.

Sample	I_{corr}, A/cm^2	E_{corr}, V
Low carbon steel	1.16×10^{-4}	−0.66
Ti-Mo coated	1.95×10^{-5}	−0.351

4. Conclusions

From the above discussions, it can be concluded that:

- (1) A dense, no pore Ti-Mo coating with about 300 μm in thickness has been successfully and homogeneously deposited on the surface of low carbon steel by laser cladding.
- (2) The XRD analysis showed that the crystal structures of the coatings were consisted of Fe_2Ti phase and β-Ti phase, while Mo stays mainly in the β-Ti.
- (3) The microhardness of the coating was enhanced to 1000 $HV_{0.5}$, could be improved as much as 4.5 times after laser cladding and the value of microhardness decreased along the depth.
- (4) Electrochemical polarization results have proven that the corrosion resistance of low carbon steel has been improved by the Ti-Mo coating.

Acknowledgements

This project was supported by the Scientific and Technological Achievements Transformation and Industrialization of Beijing Municipal Education Commission, the Suzhou Municipal Science and Technology Plan Project (Grant No.SYG201002), the National Natural Science Foundation of China (Grant No.51101056) and National Science & Technology Pillar Program (Grant No.2011BEA12B03).

References

[1] T. M. Yue, J.K. Yu, Z. Mei, H.C. Man, *Materials Letters* 2002; 52: 206-212.

[2] Z. Sun, I. Annergren, D. Pan, T.A. Mai, *Mater. Sci. Eng. A* 2003; 345: 293-300.

[3] Lore Thijs, Frederik Verhaeghe, Tom Craeghs, Jan Van Humbeeck, Jean-Pierre Kruth, *Acta Materialia* 2010; 58: 3303-3312.

[4] J.E.G. González and J.C. Mirza-Rosca, *J. Electroanal. Chem*.1999; 471: 109–115.

[5] D. Kuroda, M. Niinomi, M. Masahiko, Y. Kato and T. Yashiro, *J. Biomed. Mater. Res*. 1995; 29: 943–950.

[6] M. Niinomi, D. Kuroda, K. Fukunaga, M. Morinaga, Y. Kato, T. Yashiro and A. Suzuki, *Mater. Sci. Eng. A* 1999; 263: 193–199.

[7] W.F. Ho, C.P. Ju and J.H. Chern Lin, *Biomaterials* 1999; 20: 2115–2122.

[8] M. Sugano, Y. Tsuchida, T. Satake and M. Ikeda, *Mater. Sci. Eng. A* 1998; 1-2: 163–168.

[9] H. Guo and M. Enomoto, *Scripta Materialia* 2006; 54: 1409–1413.

[10] E. Sukedai, D. Yoshimitsu, H. Matsumoto, H. Hashimoto and M. Kiritani, *Mater. Sci. Eng. A* 2003; 1-3: 133–138.

[11] Y. Liu, W.F. Wei, K.C. Zhou, F. Chenl and H.P. Tang, *J. Central South Univ. Technol*. 2003; 2: 81–86.

[12] L.C. Zhang, T. Zhou, M. Aindow, S.P. Alpay, M.J. Blackbur and M.H. Wu, *J. Mater. Sci*. 2005; 40: 2833–2836.

[13] Petzow G. Metallographic etching: techniques for metallography, ceramography, plastography. *Materials Park (OH)*: *ASM International*, 1999.